

Two-parameter liquid drop describing symmetric fission

Xu Shuwei and Wang Zhengda

Institute of Modern Physics, Academia Sinica, Lanzhou, The People's Republic of China

(Received 31 July 1987)

A two-parameter liquid drop model has been proposed to describe the symmetric fission process by using generalized Cassinian ovals as the function family of nuclear surface shapes. The saddle-point shapes and other properties have been calculated over a wide range of the fissility parameter x and compared with those using other methods. The agreement is surprisingly good. With the aid of an adiabatic approximation, the scission-point configurations for $0.3 < x < 0.67$ have been determined, and the mutual potential energies at the scission point were calculated and are consistent with the experimental data for the most probable value of the total fission-fragment kinetic energy. The simple model has been extended to asymmetric systems, and, therefore, can be used in dynamical calculations for nuclear systems with large deformation.

INTRODUCTION

Some interesting subjects associated with fission processes are the predictions of saddle-point and scission-point configurations as well as the calculations of fission barrier and the total kinetic energy of fission-fragments in a framework of a liquid drop model. The prediction of the equilibrium configuration at the saddle point is probably the most important among them. A very well known result for symmetric fission was obtained by Cohen and Swiatecki¹ and Strutinsky *et al.*² independently in 1963. The mathematical methods used by the two groups are somewhat different, but in general the results are in good agreement. Since then the results of Ref. 1 have been quoted by others extensively, in which the variation of the radial variable of nuclear surface from the radius of undistorted sphere was expressed in terms of a spherical harmonic expansion with nine lowest even order terms. Nine parameters, of course, are too much for dynamical calculations. A nuclear surface family with three symmetric degrees of freedom was tested by Nix and Swiatecki³ in 1965, which was specified in terms of two spheroids connected by a smoothly joined quadratic surface of revolution. They found that all the saddle-point properties were reproduced with amazing accuracy. For example, over the entire range of fissility x , the calculated fission barriers are accurate to within one-half an MeV. In addition, Lawrence⁴ calculated the equilibrium configuration in terms of two free parameters without explicit physical meaning. It, however, works only for the region of $x > 0.7$. In 1968, Stavinsky *et al.*⁵ described the nuclear shapes by using Cassinian ovals which reproduced the saddle-point shape and fission barrier well for x values between 0.5 and 1.0. Based on the single parameter model, as x decreases the equilibrium shape will be elongated monotonously. The behavior is different from Cohen and Swiatecki's prediction that the elongation of the equilibrium shape increases firstly and then decreases. In 1980 Trentalange *et al.*⁶ presented a truncated Legendre polynomial in cylindrical coordinates

for defining axially symmetric shapes, which is particularly appropriate for describing elongated and multineck configurations. The shape parametrization introduced by Trentalange *et al.* with eight symmetric degrees of freedom is substantially more accurate than that of Cohen and Swiatecki for values of x below 0.7. In comparison with the earlier calculations, the Legendre-polynomial version with eight parameters gives the best results of symmetric fission barrier for x in the range from 0.15 to 1.00. Recently extensive investigations of heavy ion induced reactions, quantitative description of fusion fission, quasifission, and fast fission processes all require a simple way to describe the nuclear shapes in the dynamical process for large deformed nuclei quantitatively. A couple of simple approaches have been tested so far; however, they are not very satisfactory.^{7,8} In this paper a two-parameter model has been found to be accurate enough to describe the nuclear shapes in fission process. It may be used as a basis for dynamical calculations of the nuclear system with a large deformation.

STATIC POTENTIAL SURFACE CALCULATION

We consider the family of nuclear surfaces described in the cylindrical coordinates (ρ, z, φ) by

$$k_\rho^2 \rho^2 = (a^4 + 4c^2 k_z^2 z^2)^{1/2} - (c^2 + k_z^2 z^2), \quad (1)$$

where k_ρ , k_z are called radial and axial press coefficient, respectively. The requirement of constant volume is utilized to eliminate the constant a and to keep $k_\rho^2 k_z^2 = 1$, so that Eq. (1) describes a two-parameter function family of the possible shapes of a liquid drop. The distance between the centers of mass of two fragments can be analytically written as

$$R_{12} = \frac{a}{4k_z} \left[\frac{a}{R_0} \right]^3 (3 - \varepsilon^4), \quad (2)$$

where R_0 is the radius of undistorted spherical nucleus, and $\varepsilon = c/a$. The quantities R_{12} , k_z were selected as free

parameters because of their explicit physical meaning. The potential surfaces for different x values were calculated in the two-dimensional space (R_{12}, k_z) . It should be noted that the family described by Eq. (1) is a generalized Cassinian oval. The family becomes Cassinian ovals when $k_\rho = k_z = 1$. Actually, k_ρ and k_z are nothing but a set of linear transformation coefficients of coordinates ρ and z .

Stavinsky's⁵ method was modified and used to calcu-

late the Coulomb energy and the surface energy of a uniformly charged liquid drop. The integral representation of the Coulomb energy relative to that of an undistorted sphere is

$$B_c = \frac{3}{4\pi A^{5/3}} \int_0^{z_+} dz_1 \left[\frac{z_1}{2} \frac{d\rho_1}{dz_1} - \rho_1^2 \right] \phi(\rho_1, z_1) \quad (3)$$

and $\phi(\rho_1, z_1)$ is given by

$$2 \int_{z_-}^{z_+} \frac{1}{g_{12}} \left[\left(\rho_2^2 + \frac{g_{12}^2}{4} (k_{12}^2 - 2) + (z_1 - z_2) \frac{1}{2} \frac{\partial \rho_2^2}{\partial z_2} \right) K(k_{12}^2) + \frac{1}{2} g_{12}^2 E(k_{12}^2) \right] dz_2, \quad (4)$$

where

$$g_{12}^2 = (\rho_1 + \rho_2)^2 + (z_1 - z_2)^2,$$

$$k_{12}^2 = 4\rho_1\rho_2/g_{12}^2,$$

$$z_{\pm} = \pm(a^2 + c^2/k_z)^{1/2},$$

A is the mass number of the nucleus and $K(k_{12}^2)$, $E(k_{12}^2)$ are the complete elliptic integrals of the first and second kinds, respectively, and are evaluated by using the polynomial approximation of Ref. 9. The integral representation of the surface energy relative to that of the sphere is

$$B_s = \frac{a^2 k_z}{A^{2/3}} \int_0^{z_{\max}} \left[(1 - k_z^3) \rho^2 + k_z^3 \left(\frac{(1 + 4\epsilon^2 z^2)^{1/2} - \epsilon^2}{1 + 4\epsilon^2 z^2} \right) \right] dz, \quad (5)$$

where $z_{\max} = (1 + \epsilon^2)^{1/2}$.

Equations (3) and (4) are evaluated on the VAX-11/780 computer by Legendre-Gauss quadrature. The interval of each onefold integral was divided into 16 subintervals. The integral in each subinterval was evaluated using fourth order Legendre-Gauss quadrature. Each twofold integration of Coulomb energy required 10 sec of computer time. The calculated results of Coulomb energy

and surface energy for a sphere and two spheroids compared with those of Cohen and Swiatecki's and Lawrence's are shown in Table I. It can be seen that the accuracy of the Coulomb and surface energy evaluation is better than one part of 10^6 and one part in 10^7 , respectively. Some of Coulomb energy integrals with respect to the nuclear shapes close to scission point were also tested by using both Legendre-Gauss quadrature and Simpson's

TABLE I. Calculated values of relative Coulomb and surface energies with comparable figures for other authors.

Author	Gauss order or number of grid points	Sphere	Spheroid	Spheroid
			$\frac{\text{major axis}}{\text{minor axis}} = -\frac{1}{0.7}$	$\frac{\text{major axis}}{\text{minor axis}} = -\frac{1}{0.5}$
Relative Coulomb energy B_c				
Lawrence	Exact	1.000 000 000	0.988 678 870	0.957 975 925
	16	0.999 999 707	0.988 678 577	0.957 975 557
	96	0.999 999 998	0.988 678 869	0.957 975 925
Cohen and Swaitecki	41	0.999 998 2	0.988 676 6	
	61	0.999 999 3	0.988 678 4	
This paper	16×4	0.999 999 8	0.988 678 3	0.957 975 3
Relative surface energy B_s				
Lawrence	Exact	1.000 000 000	1.021 383 583	1.076 728 262
	16	1.000 000 000	1.021 383 583	1.076 728 262
This paper		1.000 000 0	1.021 383 5	1.076 728 2

rule in which the tolerance was set to 2×10^{-6} . The results by both ways are within the relative error 2×10^{-6} . In short, the evaluation of Coulomb energy is accurate enough to determine saddle-point and scission-point properties very well. The typical calculated contour maps of the potential surface in the region of the saddle point are shown in Fig. 1. The shape evolution from the spherical nucleus to the scission-point configuration near the fission potential valley is shown in Fig. 2.

There is an explicit analytical relation between the axial press coefficient k_z and the radius of the neck joining one fragment to another b

$$b^2 = a^2(1 - \varepsilon^2)k_z. \quad (6)$$

Because the conservation of volume, the volume of the liquid drop can be written as

$$\frac{4}{3}\pi R_0^3 = V = \pi a^3 \left[\frac{(1 + \varepsilon^2)^{1/2}}{3} (1 - 2\varepsilon^2) + \frac{1}{2\varepsilon} \text{arsh} 2\varepsilon(1 + \varepsilon^2)^{1/2} \right]. \quad (7)$$

Therefore, the radius of neck can be easily used as a free parameter instead of k_z , and the above calculated results can be displayed in the two-dimensional space (R_{12}, b) .

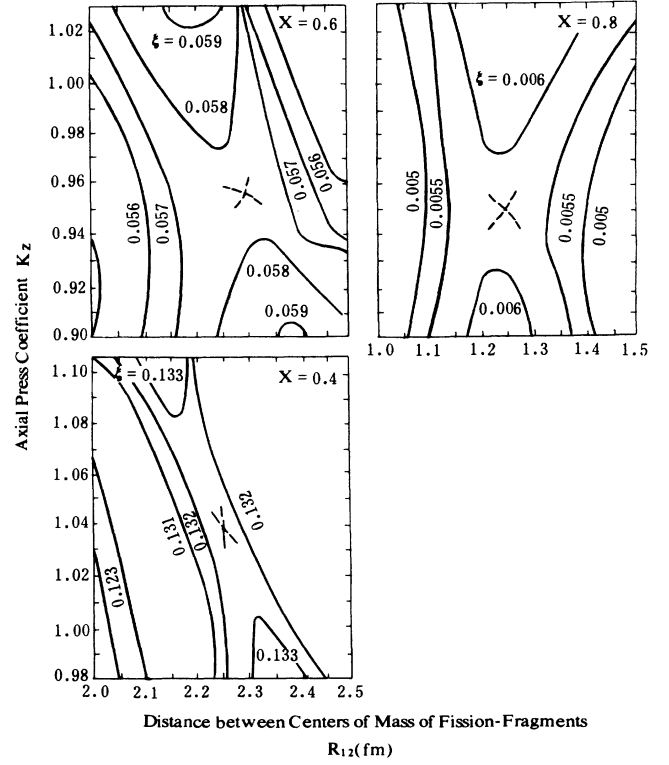


FIG. 1. Contour maps of potential energy near the saddle point for the nuclei with $x=0.4, 0.6$, and 0.8 .

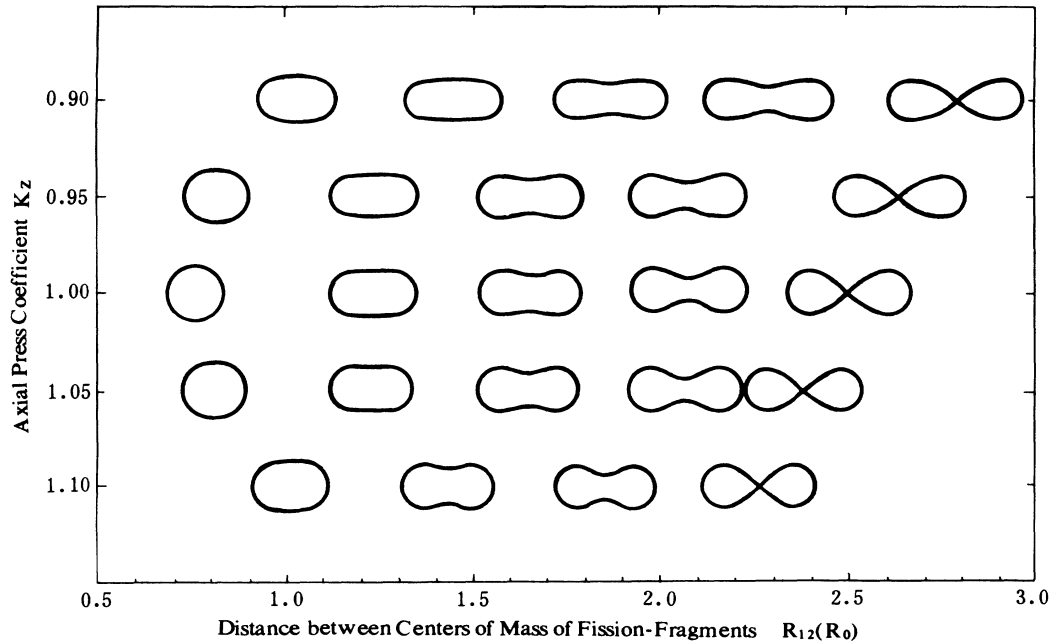


FIG. 2. Evolution of the shapes of nuclear surface near the fission potential valley on a $k_z - R_{12}$ map. The figures are rotational symmetry about horizontal axis.

SADDLE-POINT DETERMINATION AND SADDLE-POINT PROPERTIES CALCULATIONS

The exact position of saddle point was determined in the following way. First, we determined the maximum value in the potential energy surface of the two-dimensional space (R_{12}, k_z) by means of the method of parabolas as the k_z was fixed. Different maximum values were obtained for different values of k_z . Secondly, the minimum value among the above maximum points was determined by the method of parabolas also. The energy

difference between the determined minimum value and the potential energy of the undistorted spherical nucleus is then the classical fission threshold or fission barrier. In the meantime the shape parameters, the relative Coulomb energy, and the relative surface energy of the saddle point are obtained. For each saddle point the following quantities were evaluated by using the shape parameters: the parallel moment of inertia J_{\parallel} , the perpendicular moment of inertia J_{\perp} , the inverse of the effective moment of inertia J_{eff} , and the quadrupole moment Q . The J_{\parallel} is computed by the expression

$$J_{\parallel} = \frac{15}{8} \left[\frac{a}{R_0} \right]^5 k_z \left[(1 + \varepsilon^4) z_{\max} + 2\varepsilon^2 z_{\max}^3 + \frac{1}{5} z_{\max}^5 - \varepsilon^2 z_{\max} S_q \right. \\ \left. - \frac{\varepsilon}{2} \ln(2\varepsilon z_{\max} + S_q) - \frac{Z_{\max}}{8\varepsilon^2} S_q^3 + \frac{Z_{\max}}{16\varepsilon^2} S_q + \frac{1}{32\varepsilon^3} \ln(2\varepsilon z_{\max} + S_q) \right], \quad (8)$$

where $S_q = (4\varepsilon^2 z_{\max}^2 + 1)^{1/2}$. The J_{\perp} is given by

$$J_{\perp} = \frac{J_{\parallel}}{2} + \frac{15}{8} \left[\frac{a}{R_0} \right]^5 \frac{1}{k_z^2} \left[\frac{z_{\max}}{8\varepsilon^2} S_q^3 - \frac{z_{\max}}{16\varepsilon^2} S_q - \frac{1}{32\varepsilon^3} \ln(2\varepsilon z_{\max} + S_q) - \frac{2}{3} \varepsilon^2 z_{\max}^3 - \frac{2}{5} z_{\max}^5 \right]. \quad (9)$$

The J_{eff} and Q are evaluated with the expressions

$$J_{\text{eff}} = \frac{1}{J_{\parallel}} - \frac{1}{J_{\perp}}, \quad (10)$$

$$Q = \frac{16}{15} \pi (J_{\perp} - J_{\parallel}). \quad (11)$$

Cohen and Swiatecki's definition of the saddle-point properties in Eqs. (8)–(11) were adopted to facilitate comparison with their work.

CALCULATED RESULTS ABOUT SADDLE-POINT CONFIGURATION AND DISCUSSION

Typical saddle-point shapes are shown in Fig. 3 and compared with those of Ref. 1. Generally speaking, both of them are in very good agreement. Looking closely, we found that the neck of the predicted saddle-point shape is a little bit smaller than that of Ref. 1 for $x=0.7$, and the predicted necks of the saddle-point shapes are slightly larger and smoother than those of Cohen and Swiatecki's for $x=0.3$ and 0.4 . The calculated saddle-point properties in our two-dimensional space and the percent difference between the calculated properties and those properties calculated by Cohen and Swiatecki are listed in Table II. The percent differences of the relative Coulomb energy and surface energy are less than 1%. The percent differences of the quadrupole are less than 6.4%. The percent differences of the parallel moment of inertia, the perpendicular moment of inertia, and the inverse of the effective moment of inertia are less than 1.5%, 5.0%, and 2.5%, respectively. So far as the fission barrier is concerned, earlier results^{1,3,6} and the results calculated using our generalized Cassinian ovals are compared and listed in Table III. In the range of $x \geq 0.3$,

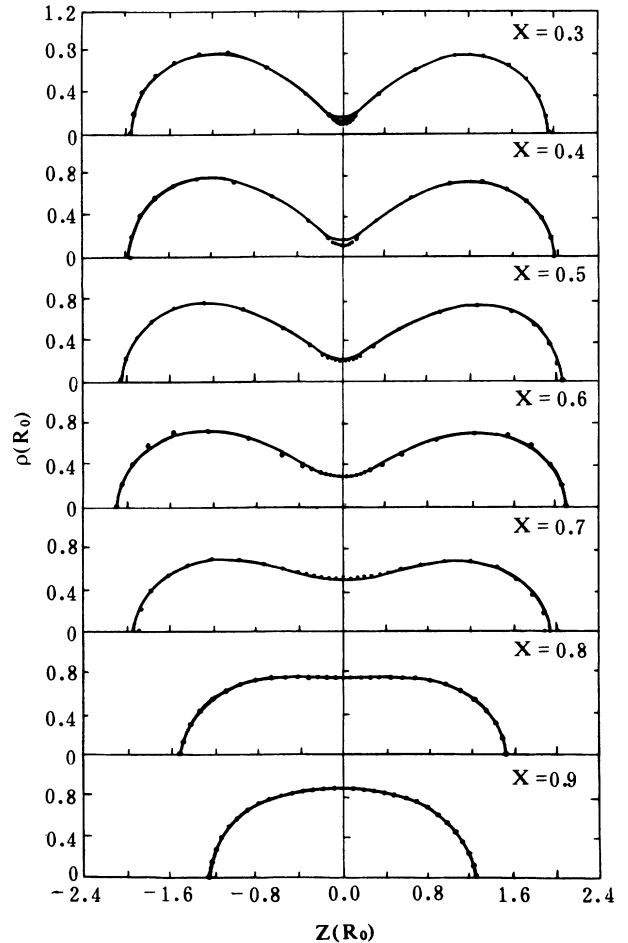


FIG. 3. Comparison of saddle-point shapes calculated in the two dimensional space (solid line) with those of Ref. 1 (point).

TABLE II. Determined saddle-point shape parameters and calculated saddle-point properties, as well as percent difference [$\delta K \equiv (K - K^{\text{CS}})/K^{\text{CS}}$] between this paper and Cohen and Swiatecki's. The superscript CS refers to Cohen and Swiatecki's paper (Ref. 1).

X	B_s (δB_s)	B_c (δB_c)	J_{\parallel} (δJ_{\parallel})	J_{\perp} (δJ_{\perp})	J_{eff} (δ_{eff})	Q (δQ)	k_z	$R_{12}(R_0)$	ϵ
0.9	1.020 08 (+0.01%)	0.989 24 (-0.01%)	0.7941 (-0.09%)	1.1907 (+0.09%)	0.4195 (+0.45%)	1.3290 (+0.45%)	0.97671	0.948 59	0.541 59
0.8	1.081 03 (+0.09%)	0.953 07 (-0.06%)	0.6222 (-0.29%)	1.6258 (+0.46%)	0.9922 (+0.77%)	3.3631 (+0.94%)	0.95071	1.23821	0.74760
0.7	1.217 39 (+0.98%)	0.861 15 (-0.92%)	0.4760 (-1.24%)	2.9948 (+5.11%)	1.7669 (+2.49%)	8.4404 (+6.40%)	0.923 09	1.872 84	0.920 47
0.6	1.281 78 (-0.45%)	0.813 39 (+0.48%)	0.4902 (-0.14%)	4.0563 (-2.81%)	1.7934 (-0.24%)	11.9502 (-3.17%)	0.955 67	2.288 32	0.980 92
0.5	1.281 39 (-0.40%)	0.813 92 (+0.63%)	0.5210 (-0.19%)	4.0038 (-3.82%)	1.6697 (-0.35%)	11.6710 (-4.35%)	1.000 00	2.286 49	0.990 04
0.4	1.278 40 (-0.14%)	0.817 36 (+0.20%)	0.5484 (-0.76%)	3.8606 (-1.24%)	1.5644 (0.11%)	11.0990 (-1.44%)	1.041 58	2.248 10	0.994 67
0.3	1.276 12 (-0.08%)	0.820 48 (+0.03%)	0.5706 (+0.87%)	3.7318 (-0.39%)	1.4846 (-1.09%)	10.5933 (-0.61%)	1.075 57	2.210 22	0.997 53

Trentalange's results are better than ours, but the maximum difference between them is less than 0.6 MeV. In comparison with Nix's results, our parametrization works worse for $x \leq 0.7$ but better for $x > 0.7$. The fission barriers given by our parametrization are higher for $0.55 \leq x \leq 0.8$, but lower for $0.3 \leq x < 0.55$ than those given by Cohen and Swiatecki. Therefore, our predicted saddle-point shapes for $x = 0.3$ and 0.4 are more realistic than Cohen and Swiatecki's. It should be pointed out that the generalized Cassinian ovals cannot describe the configuration of two touching spheres, and that consequently the calculated saddle-point energies will be too high for $x \leq 0.2$.

DETERMINATION OF SCISSION-POINT AND MUTUAL POTENTIAL AT SCISSION

The scission point in the static potential surface was determined by means of the adiabatic approximation.

The system starts to climb along the fission potential valley, over its saddle point, goes further, and reaches a certain distance between the centers of mass R_{12} , where the minimum of potential energy of the system in the direction of coefficient k_z disappears. At that distance, the potential energy of the system slides down monotonously as the k_z increases, and the system descends to scission. The determined scission-point shapes for $x \geq 0.3$ are nearly indistinguishable with respect to different fissilities, if the radius of the undistorted spherical nucleus is used as the unit of length. The parameters of scission-point shapes k_z for different nucleus are close to 1.05. A typical scission-point shape is shown in Fig. 4. In principle, scission points cannot be determined from static potential-energy surface alone, but instead require a consideration of nuclear dynamics. For x values less than 0.67, however, the neck is well developed at the saddle point and the scission configuration is fairly close to the saddle configuration. The influence of the dynamical pro-

TABLE III. Fission barriers calculated using four different parametrizations.

X	Nix and Swiatecki			
	Cohen and Swiatecki spherical harmonic (nine parameters)	three quadratic surfaces (three parameters)	Trentalange <i>et al.</i> Legendre polynomial (eight parameters)	Present work generalized Cassinian ovals (two parameters)
0.1		0.233 63	0.233 71	
0.2		0.202 17	0.202 14	
0.3	0.169 24	0.168 14	0.167 91	0.168 41
0.4	0.132 84	0.132 36	0.131 90	0.132 29
0.5	0.095 35	0.095 27	0.094 64	0.095 30
0.6	0.056 95	0.057 47	0.056 74	0.057 85
0.7	0.022 36	0.022 93	0.022 37	0.023 00
0.8	0.005 91	0.006 05	0.005 91	0.005 94
0.9	0.000 71	0.000 73	0.000 71	0.000 71

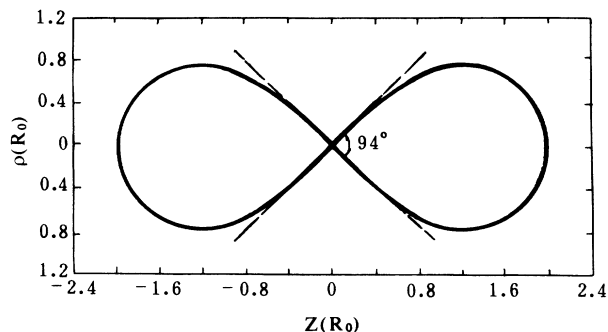


FIG. 4. Shape of the scission-point configurations determined with the aid of adiabatic approximation for $x \geq 0.3$.

cess from saddle point to scission point on the nuclear scission can be ignored. The adiabatic approximation is acceptable to determine the scission-point shapes for the nuclei with $x < 0.67$. The fact that for those x values almost all of the kinetic energy of the fragments is acquired by post-scission acceleration of the fragments in mutual interaction fields has been verified by Nix's dynamical calculation.¹⁰ On the other hand, the insensitivity of the kinetic energy release in the fission process to excitation energy of the compound nucleus was observed very early. A number of experimental data^{11,15} show that the average total kinetic energy of the fragments from fusion-fission process almost keeps a constant within the experimental error as the incident energy is changed a lot. This means that the combination of the various factors of the compound nucleus, such as temperature, rotation, and so on, has very little effect on the collective motion in the fission degree of freedom. For $x < 0.67$, the static mutual potential at the scission point can be, therefore, used for estimating the total kinetic energy of the fragments.

The dominant part of the mutual potential is Coulomb potential (Ec), which is calculated easily according to the determined geometrical shape at the scission point in Fig. 4. It turns out that $Ec = 0.186Ec^{(0)}$, where $Ec^{(0)}$ is the Coulomb energy of the undistorted sphere. Finally, $Ec = 0.131Z^2/A^{1/3}$, when we use the radius parameter value 1.2249 fm. Z, A are the charge number and mass number of compound nucleus, respectively. The mutual nuclear potential at the scission point is relatively small, but rather difficult to estimate because of the shapes of the fragments. A semiempirical approach has been proposed, which was tested for the nuclear interaction between two spherical nuclei and then extended to the case between two nuclei with any geometrical shape (see Appendix). The estimated values of the mutual nuclear potential are somewhere between -3 and -4 MeV. The comparison of calculated mutual potential energy, including Coulomb and nuclear potential, with experimental data of the most probable value of the fission-fragments kinetic energy for $0.33 < x < 0.67$ is shown in Fig. 5, from which a good agreement can be seen. Presumably, the shape parametrization is reasonable near the scission-point region.

EXTENDING TO ASYMMETRIC SYSTEM

Cassianian ovals has been extended to describe asymmetric liquid drop in 1971 by Pashkevish¹⁸ and Adeev

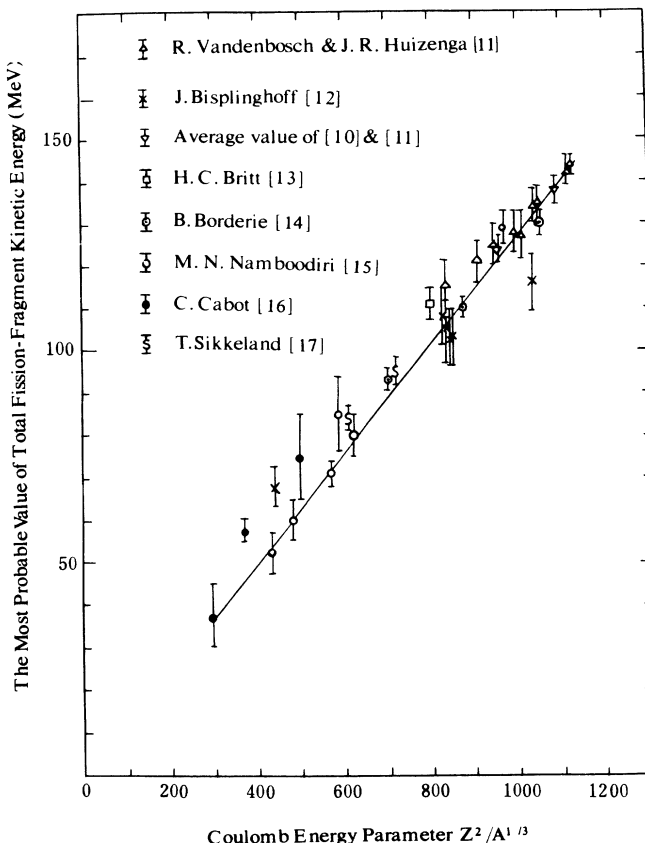


FIG. 5. Comparison of calculated mutual potential energies, including Coulomb and nuclear potential, with experimental data (Refs. 11-17) of the most probable value of the total fission-fragment kinetic energies of the fission fragments for $0.33 < x < 0.67$.

et al.,¹⁹ respectively. In Pashkevish's paper the new coordinates (R, x) have been introduced such that the coordinate line $R = \text{const}$ is a Cassianian oval. In order to describe asymmetric shapes R was simply replaced with $R_0[1 + \alpha p_1(x)]$, where $p_1(x)$ is the first order Legendre polynomial. The extension in Adeev's paper was more complicated, but gave more general results. The fission barriers of liquid drop for some heavy nuclei have been calculated in both papers. Their results show that the calculated fission barriers of liquid drop from asymmetric process are higher than those for corresponding symmetric process. The difference of the calculated fission barriers between asymmetric and symmetric process varies in the range from 1.0 to 2.0 MeV, and depends on the system and its asymmetry. However, the asymmetric process became energetically favorable when the shell correction was taken into account by means of the Strutinsky method.²⁰

We add a cubic expression of z into the first term of the right side of Eq. (1),²¹ namely

$$k^2 \rho^2 = (a^4 + 4c^2 k_z^2 z^2 + ck_a k_z^3 z^3)^{1/2} - (c^2 + k_z^2 z^2), \quad (12)$$

which can be used to describe the shapes of asymmetric system. The constant k_a is restricted by the asymmetry of the system, so that Eq. (12) is also a two-parameter function family of the possible shapes of a liquid drop. In

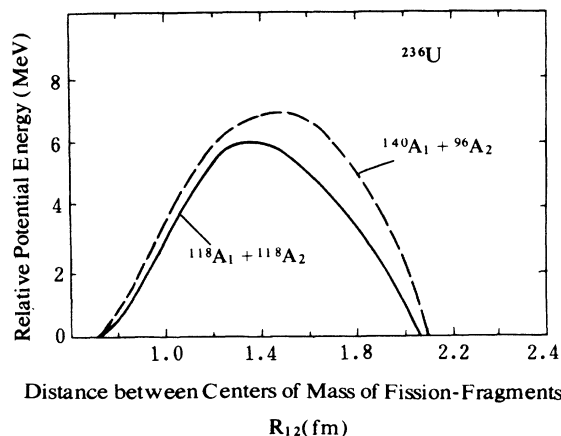


FIG. 6. Relative potential energy for the nucleus ^{236}U as a function of distance between the centers of mass of fission fragments via symmetric path (solid line) and asymmetric path (dashed line).

this case, Eq. (6) is still satisfied. The radius of the neck b which plays a very important role in describing heavy ion induced reaction is still able to be used as a free parameter naturally in the asymmetric process. Taking ^{236}U as an example and using a method similar to the mentioned above Eqs. (1)–(6), we evaluated the static potential-energy surfaces for both symmetric and asymmetric processes, and then the variation of relative potential energy of the system along the fission potential valley via both symmetric and asymmetric paths. The results are shown in Fig. 6. It can be seen that the fission barrier of the asymmetric process is a little wider and about 1 MeV higher than that of symmetric process. The asymmetric process will be also energetically preferable, if the shell effect is taken into account. In addition, using adiabatic approximation and assuming uniform charge distribution of the fission fragments, we determined the scission-point shapes as a function of the mass of the fragments and hence the mutual potential energy at the scission point. The results compared with the experimental data of mean fragment total kinetic energy are shown in Fig. 7, from

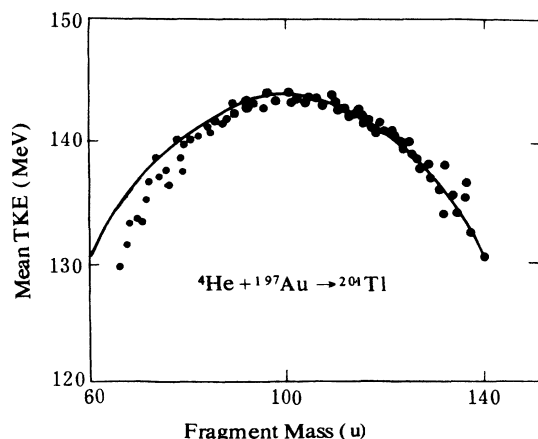


FIG. 7. Mean fission-fragment total kinetic energy as a function of fragment mass for the fission of ^{201}Tl . Solid circles are the experimental data [from Nix and Swiatecki (Ref. 3)]. Solid line is the calculated mutual potential energies at the scission point.

which good agreement can be seen. ^{201}Tl produced with the reaction $^4\text{He} + ^{197}\text{Ag}$ was taken as the compound nucleus because its $x < 0.67$, its temperature is low and angular momentum is rather small. We should be cautious, however, and not read too much into this agreement. In fact, the experimental distribution of mean fragment total kinetic energy is sensitive to the temperature of the compound nuclei, but the effect of the temperature of the compound nuclei was not taken into account at all in the adiabatic approximation. The agreement only gave a hint that the shape parametrization given by Eq. (12) will be probably used for further studying the distribution of mean fragment total kinetic energy.

SUMMARY

The proposed two-parameter model not only makes the evaluation simple, but also has a clear physical picture. One of the free parameters describing the shape of liquid drop is the distance between the centers of mass of the fission fragments. Another is the axial press coefficient, which expresses the deviation of nuclear shape from the Cassinian ovals after a linear coordinate transformation and can be easily replaced by the radius of neck. Over a wide range of x the shapes and the properties of saddle point predicted by the two parameter model are surprisingly consistent with those determined by using nine parameters in Cohen and Swiatecki's paper, and the difference between the fission barriers calculated in Trentalange's paper and in ours are less than 0.6 MeV. The predicted scission-point configurations for the nuclei of $0.3 < x < 0.67$ with the aid of adiabatic approximation are also reasonable. Furthermore, the simple model can be generalized to describe asymmetric fission process easily, and, therefore, will be helpful for the dynamical calculations of heavy ion induced fusion fission, quasifission, and fast fission processes.

ACKNOWLEDGMENTS

We are grateful to Mr. Zhang Zhen collecting the experimental data of the total kinetic energy of fission fragments and taking part in the mutual potential estimation. The authors also wish to thank Prof. C. Y. Wong and Prof. Y. T. Zhu for reading the manuscript and helpful discussions.

APPENDIX: MUTUAL NUCLEAR POTENTIAL ESTIMATION

In order to illustrate the essence of the approach, we begin with deriving the expression of the nuclear potential between a pair of spherical nuclei. A spherical nucleus is assumed to be equivalent to a set of overlapping spheres with different densities and different radii r (see Fig. 8). All component spheres possess the same center of mass as original nucleus. The density of each component is uniform and expressed by

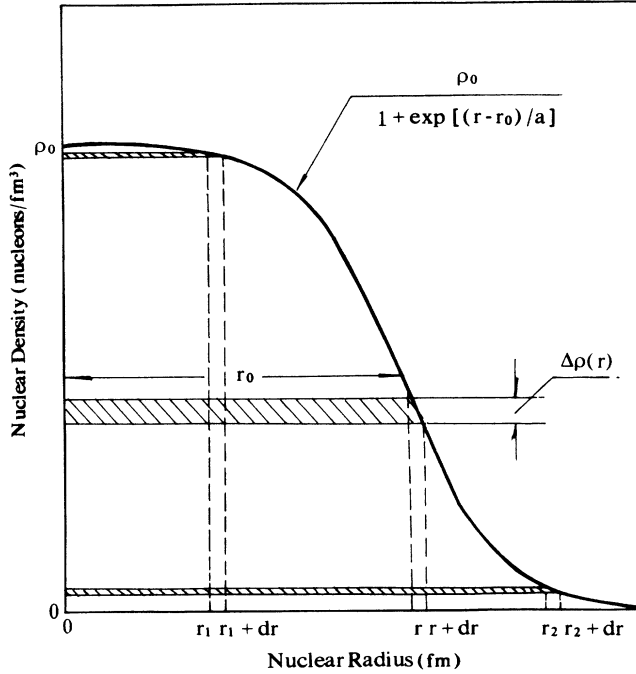


FIG. 8. Schematic diagram of a spherical nucleus formed of a set of component spheres, where r and $\Delta\rho(r)$ represent the radius and density of a certain component sphere.

$$\Delta\rho(r) = \frac{\rho_0 \exp[(r - r_0)/a] dr}{a \{1 + \exp[(r - r_0)/a]\}^2}. \quad (\text{A1})$$

The sum of all the component densities is just equal to the Fermi density distribution of original nucleus, namely

$$\int_r^\infty \frac{\rho_0 \exp[(r - r_0)/a] dr}{a \{1 + \exp[(r - r_0)/a]\}} = \frac{\rho_0}{1 + \exp[(r - r_0)/a]}, \quad (\text{A2})$$

where a , r_0 , and ρ_0 are the diffuseness, half-density radius, and the saturated density of the nucleus, respectively. Based on the experimental results of high energy electron scattering,^{22,23} parameter values $a=0.54$ fm and $r_0=1.1$ A fm are used. It can be seen from Eq. (A1) that the density of component sphere depends on the radius difference $\Delta r = r - r_0$ only. Even in two unequal nuclei there exist one-to-one component spheres with equal density, which are called the component pairs with equal density. A component pair with equal density will not interact each other unless they overlap. The interaction between an overlapping component pair with equal density is proportional to their density and the decreasing of external surfaces of the two components owing to their

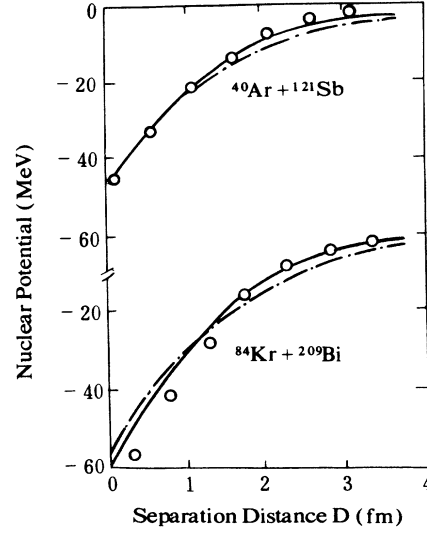


FIG. 9. Estimated nuclear potential (dashed lines) between ^{40}Ar and ^{121}Sb as well as ^{84}Kr and ^{209}Bi as a function of separation distance $D = R_{12} - r_0^{(1)} - r_0^{(2)}$, compared with the results calculated using the proximity theorem (dots) and energy-density formalism (solid lines).

overlapping.²⁴ The latter is given by

$$S = 4\pi d \frac{r_1 r_2}{r_1 + r_2},$$

where r_1 and r_2 are the radii of the two components, d the overlapping length of the component pair with equal density on the line linking the centers of mass. The nuclear potential, caused by the interaction between the diffuse tails of two nuclei, is assumed to be proportional to the sum of all the nuclear interactions between every overlapping component pair with equal density in the two nuclei because the saturation of nuclear force. If $r_0^{(1)}$ and $r_0^{(2)}$ are the half-density radii of the two nuclei, and D is the separation distance between the two nuclei, the radii of the minimum overlapping component pair with equal density are $r_0^{(1)} + D/2$ and $r_0^{(2)} + D/2$, because this pair of radii corresponds to equal radius difference, $\Delta r_1 = \Delta r_2 = D/2$, and the sum of them is just equal to the distance between the centers of mass of the two nuclei, $r_0^{(1)} + r_0^{(2)} + D$. Starting from this pair of minimum radii we made up all the overlapping component pairs with equal density by enlarging r_1 and r_2 while keeping $\Delta r_1 = \Delta r_2$. It follows from the above assumptions that the nuclear potential at the separation distance $D = 2R - 2r_0^{(1)}$ can be written as

$$U_n(2R - 2r_0^{(1)}) = 4\pi(\gamma_1 + \gamma_2)N_0 \int_R^\infty (r_1 - R) \frac{r_1(r_1 + r_0^{(2)} - r_0^{(1)})}{2r_1 + r_0^{(2)} - r_0^{(1)}} \frac{\exp[(r - r_0^{(1)})/a] dr_1}{a \{1 + \exp[(r - r_0^{(1)})/a]\}^2}, \quad (\text{A3})$$

where γ_1 and γ_2 are the surface-tension coefficients of both nuclei, N_0 is a constant related to the saturation of nuclear force. When we estimated the nuclear potential for a touching configuration of two spherical liquid

drops, the parameter value $R = 1.2249 \text{ A}^{1/3}$ fm was taken, which corresponds to the sharp edge. The nuclear potential as a function of separation distance for heavy and mediate-heavy systems were calculated by means of

Eq. (A4) systematically, which fit proximity potential well when the parameter value $N_0 = 1.85$ was used. The typical results for $^{40}\text{Ar} + ^{121}\text{Sb}$ and $^{84}\text{Kr} + ^{209}\text{Bi}$ compared those predicted by proximity function and energy density formalism,²⁵ are shown in Fig. 9. It indicates that the assumption about equivalent component pairs with equal density is reasonable.

A similar procedure can be made by estimating the nuclear potential between two nuclei with any geometric

shapes. The half-density radius is no longer a constant, but a function of θ and φ instead. The component drops are still the similar figures of original liquid drop and have the same center of mass as original nucleus. The density of the component drop no longer depends on the separation radius itself, but depends on its projection on the line linking the centers of mass. A general expression of nuclear potential between the two nuclei is obtained

$$U_n(2R - 2r_0^{(1)}) = \frac{\gamma_1 + \gamma_2}{2} N_0 \int_R^\infty S(R, r_1, r_0^{(1)}(\theta_1, \varphi_1), r_0^{(2)}(\theta_2, \varphi_2)) \frac{\exp[(r - r_0^{(1)})/a] dr_1}{a \{1 + \exp[(r - r_0^{(1)})/a]\}^2}, \quad (\text{A4})$$

where $r_0^{(1)}$ and $r_0^{(2)}$ are the half-density radii of both nuclei on the line of the centers of mass, r_1 the radial distance from the center of mass of a component drop to its surface along the line of centers of mass, and $S(R, r_1, r_0^{(1)}(\theta_1, \varphi_1), r_0^{(2)}(\theta_2, \varphi_2))$ the decreasing of external surfaces of the two components when they overlap, which, of course, depends on the shape of the liquid drop.

Since the density of the component drop decreases rapidly with its surface radial variable r_1 increasing; namely, the nuclear potential mainly depends on the interaction in the closest approach region between the two fragments, it is accurate enough that $R + 7a$ is taken as the upper limit of the integral (A4). For evaluation of the integral (A4), a pair of cones with vertex angle 94° is, therefore, taken instead of the scission-point shape in Fig. 4. When two cones overlap each other, the decreasing of their external surfaces owing to overlapping is given by

$$S = \frac{\pi}{2} \frac{\text{tg}(\delta/2)}{\cos(\delta/2)} d^2,$$

where δ is the vertex angle of the cone, and d the overlapping length of the two cones on their symmetrical axial. The mutual nuclear potential at the scission point is approximately expressed by

$$U_n(2R - 2r_0) = 2\pi\gamma N_0 \frac{\text{tg}(\delta/2)}{\cos(\delta/2)} \times \int_R^\infty (r - R)^2 \frac{\exp[(r - r_0)/a]}{a \{1 + \exp[(r - r_0)/a]\}^2}, \quad (\text{A5})$$

where $\delta = 94^\circ$, $N_0 = 1.85$, and $R = 1.2249 A^{1/3}$ fm corresponding to the sharp edge of the liquid drop. The estimated values of the nuclear potential at the scission points for $0.33 < x < 0.67$ are between -3 and -4 MeV.

- ¹S. Cohen and W. J. Swiatecki, *Ann. Phys. (N.Y.)* **22**, 406 (1963).
- ²V. M. Strutinsky, N. Ya. Lyashchenko, and N. A. Popov, *Nucl. Phys.* **46**, 639 (1963).
- ³J. R. Nix and W. J. Swiatecki, *Nucl. Phys.* **71**, 1 (1965).
- ⁴J. N. P. Lawrence, *Phys. Rev. B* **139**, 1227 (1965).
- ⁵V. S. Stavinsky, N. S. Rabotnov, and A. A. Seregin, *At. Phys. (Russian)* **7**, 1051 (1968).
- ⁶S. Trentalange, S. E. Koonin, and A. J. Sierk, *Phys. Rev. C* **22**, 1159 (1980).
- ⁷W. J. Swiatecki, *Phys. Scr.* **24**, 113 (1981).
- ⁸H. T. Feldmeier, Argonne National Laboratory Report No. ANL-PHY-85-2.
- ⁹M. Abramowitz and I. A. Stegun, *Handbook of Mathematical Functions with Formulas, Graphs, and Mathematical Tables* (U.S. GPO, Washington, D.C., 1966), p. 591.
- ¹⁰J. R. Nix, *Nucl. Phys.* **A130**, 241 (1969).
- ¹¹R. Vandenbosch and J. R. Huizenga, *Nuclear Fission* (Academic Press, New York, 1973), Table X-1, p. 290.
- ¹²J. Bisplinghoff, P. Divad, M. Blann, W. Scobel, T. Mayer-Kuckuk, J. Ernst, and A. Mignerey, *Phys. Rev. C* **17**, 177 (1978).
- ¹³H. C. Britt, B. H. Erkkila, R. H. Stokes, H. H. Gutbrod, F.

- Plasil, R. L. Ferguson, and M. Blann, *Phys. Rev. C* **13**, 1483 (1976).
- ¹⁴B. Borderie, F. Hanappe, C. Ngo, J. Peter, and B. Tamain, *Nucl. Phys.* **A220**, 93 (1974).
- ¹⁵M. N. Namboodiri, J. B. Natowitz, E. T. Chulick, K. Das, and L. Webb, *Nucl. Phys.* **A252**, 163 (1975).
- ¹⁶C. Cabot, C. Ngo, J. Peter, and B. Tamain, *Nucl. Phys.* **A244**, 134 (1975).
- ¹⁷T. Sikkeland, *Phys. Lett.* **31B**, 451 (1970).
- ¹⁸V. V. Pashkevich, *Nucl. Phys.* **A169**, 275 (1971).
- ¹⁹G. D. Adeev, A. P. Cherdantsev, and I. A. Gamalya, *Phys. Lett.* **35B**, 125 (1971).
- ²⁰V. M. Strutinsky, *Nucl. Phys.* **A95**, 420 (1976); **A122**, 1 (1968).
- ²¹Xu Shuwei and Wang Zhengda, *Annual Report 1985* (Institute of Modern Physics, Academia Sinica, Lanzhou, 1985), p. 10.
- ²²R. Hofstadter, H. R. Fechter, and J. A. McIntyre, *Phys. Rev.* **92**, 978 (1953).
- ²³B. D. Hahn, D. G. Ravenhall, and R. Hofstadter, *Phys. Rev.* **101**, 1131 (1956).
- ²⁴J. Wilczynski, *Nucl. Phys.* **A216**, 386 (1973).
- ²⁵J. Blocki, J. Randrup, W. J. Swiatecki, and C. F. Tsang, *Ann. Phys. (N.Y.)* **105**, 427 (1977).